Introduction

Continuum model

Reorientation

Variational-based weak formulation

Balance laws

Numerical studies

Initial rotation

Boundary load

Volume load

Summary

A VARIATIONAL-BASED MIXED FINITE ELEMENT FORMULATION FOR LIQUID CRYSTAL ELASTOMERS

Groß M., Dietzsch J. and Concas F.

Professorship of Applied Mechanics and Dynamics

Faculty of Mechanical Engineering

ECCOMAS 2022 (in-person event) 5-9 June, 2022

Acknowledgment: This research is provided by DFG under the grant GR 3297/7-1

TECHNISCHE UNIVERSITÄT CHEMNITZ

Introduction
Continuum model
Reorientation
Variational-based weak formulation
Balance laws
Numerical studies
Initial rotation
Boundary load
Volume load
Summary

Motivation and goals

Goal 1: FE-simulation of thermal actuation of motion of LCE materials

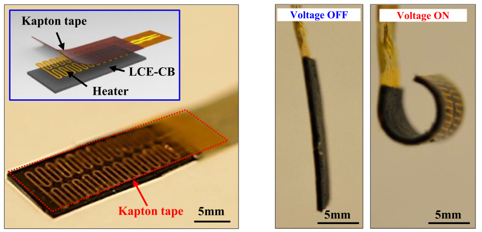

Introduction of Joule heat energy by heating pads, see Cui Y. et al. [2018]

Goal 2: FE-simulation of UV light acuation of motion of LCE materials

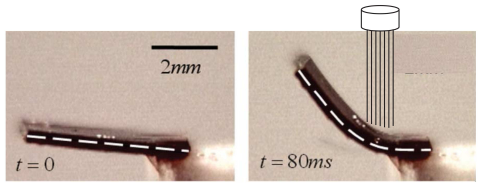

Using of UV light for inducing bending, see Corbett & Warner [2009]

Step 1: FE formulation for actuation of continuum motions by boundary or volume loads

We design a dynamic mixed FE method for continuum motions with internal reorientation

Continuum formulation with reorientation effects

(see e.g. Frank [1958], Leslie [1968], Anderson et al. [1999], Himpel et al. [2008], De Luca et al. [2013])

Continuum configurations of a LCE with orientational loads

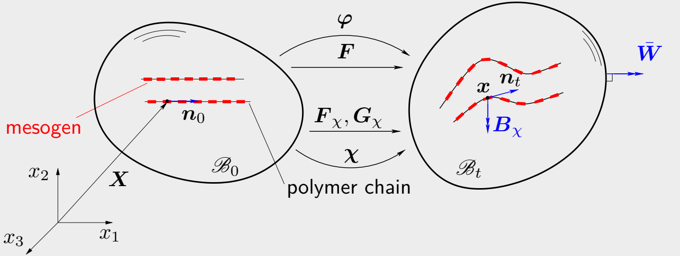

1. Orientation mapping

$$\boldsymbol{\chi} : \mathscr{B}_0 \times \mathscr{T} \rightarrow \mathbb{R}^{n_{\text{dim}}} \text{ with}$$
$$\boldsymbol{\chi}(\boldsymbol{X}, 0) = \boldsymbol{n}_0(\boldsymbol{X}) \text{ and } \boldsymbol{n}_0 \cdot \boldsymbol{n}_0 = 1$$

2. Orientation tensor

$$\boldsymbol{F}_\chi := \boldsymbol{\chi} \otimes \boldsymbol{n}_0 \qquad \boldsymbol{n}_t = \boldsymbol{F}_\chi\, \boldsymbol{n}_0$$

3. Orient. deformation tensor

$$\boldsymbol{C}_\chi := \boldsymbol{F}^t\, \boldsymbol{g}\, \boldsymbol{F}_\chi = \boldsymbol{F}^t\, \boldsymbol{g}_\chi\, \boldsymbol{F}$$

4. Distorsion tensor

$$\boldsymbol{K}_\chi := \boldsymbol{F}^t\, \boldsymbol{g}\, \boldsymbol{G}_\chi = \boldsymbol{F}^t\, \boldsymbol{g}_K\, \boldsymbol{F}$$

5. Orient. velocity vector

$$\boldsymbol{v}_\chi(\boldsymbol{X}, t) := \dot{\boldsymbol{\chi}}(\boldsymbol{X}, t) = \dot{\boldsymbol{n}}_t$$

6. Orient. momentum vector

$$\boldsymbol{p}_\chi := \rho_0 \left[(l_\chi^2 - l_0^2) \boldsymbol{A}_0 + l_0^2\, \boldsymbol{I} \right] \boldsymbol{v}_\chi$$
$$\boldsymbol{A}_0 := \boldsymbol{n}_0 \otimes \boldsymbol{n}_0$$

Polyconvex/elliptic free energy functions

(cp. Frank [1958], Leslie [1968], Warner et al. [1993], Anderson et al. [1999], Himpel et al. [2008], De Luca et al. [2013])

Free energy associated with orientational deformations

1. Interactive free energy (motivated by Anderson et al. [1999], Himpel et al. [2008])

$$\Psi_i(\boldsymbol{F}^t\,\boldsymbol{g}\,\boldsymbol{\chi}) \equiv \Psi^{\mathrm{ori}}(\boldsymbol{C}_\chi) := \hat{\Psi}^{\mathrm{ori}}(I_1^{\mathrm{ori}}, J_2^{\mathrm{ori}})$$

2. Orientational invariants

$$I_1^{\mathrm{ori}} := \boldsymbol{C}_\chi \boldsymbol{A}_0 : \boldsymbol{G}^{-1} \qquad J_2^{\mathrm{ori}} := \boldsymbol{C}_\chi \boldsymbol{A}_0 : \boldsymbol{C}_\chi \boldsymbol{A}_0$$

Free energy associated with distorsions of the orientation field

1. Frank free energy (motivated by Frank [1958], Leslie [1968], Anderson et al. [1999])

$$\Psi^{\mathrm{dis}}(\boldsymbol{K}_\chi) := \hat{\Psi}^{\mathrm{dis}}(I_1^{\mathrm{dis}}, J_2^{\mathrm{dis}})$$

2. Distorsional invariants

$$I_1^{\mathrm{dis}} := (\boldsymbol{K}_\chi - \mathrm{Grad}[\boldsymbol{n}_0]) : \boldsymbol{G}^{-1} \qquad J_2^{\mathrm{dis}} := (\boldsymbol{K}_\chi - \mathrm{Grad}[\boldsymbol{n}_0]) : (\boldsymbol{K}_\chi - \mathrm{Grad}[\boldsymbol{n}_0])$$

Free energy associated with (isothermal) elastic deformations

1. Isotropic compressible free energy (see e.g. Warner et al. [1993], Anderson et al. [1999])

$$\Psi^{\mathrm{ela}}(\boldsymbol{C}) := \hat{\Psi}^{\mathrm{ela}}(I_1^{\mathrm{ela}}, J_2^{\mathrm{ela}}, I_3^{\mathrm{ela}})$$

2. Deformation invariants

$$I_1^{\mathrm{ela}} := \boldsymbol{C} : \boldsymbol{G}^{-1} \qquad J_2^{\mathrm{ela}} := \boldsymbol{C} : \boldsymbol{C} \qquad I_3^{\mathrm{ela}} := \det[\boldsymbol{C}]$$

Reorientation with drilling degrees of freedom

Introduction
Continuum model
Reorientation
Variational-based weak formulation
Balance laws
Numerical studies
Initial rotation
Boundary load
Volume load
Summary

Reorientation modelled as dissipative process (cp. Garikipati et al. [2006])

1. Clausius-Planck inequality

$$\mathcal{D}_\chi^{\mathrm{int}} := \boldsymbol{N}_\chi : \boldsymbol{g}\,\dot{\boldsymbol{F}} - \dot{\Psi}^{\mathrm{ori}}(\boldsymbol{C}_\chi) \equiv \left[\boldsymbol{N}_\chi - \boldsymbol{F}_\chi\,\boldsymbol{S}_\chi^t\right] : \boldsymbol{g}\,\dot{\boldsymbol{F}} - \boldsymbol{F}\,\boldsymbol{S}_\chi : \boldsymbol{g}\,\dot{\boldsymbol{F}}_\chi \geq 0$$

2. Normalized orientation vectors guaranteed by drilling degrees of freedom

$$\mathbb{I}^{\mathrm{skw}} : \boldsymbol{g}\,\dot{\boldsymbol{F}}_\chi\,\boldsymbol{F}_\chi^{-1} = \boldsymbol{\epsilon}\cdot\dot{\boldsymbol{\alpha}} \qquad \dot{\boldsymbol{\alpha}} := \dot{\alpha}^k\,\boldsymbol{g}_k \circ \boldsymbol{\varphi}(\boldsymbol{X},t)$$

3. Reorientation dissipation

$$\mathcal{D}_\chi^{\mathrm{int}} := \left[\boldsymbol{N}_\chi - \boldsymbol{F}_\chi\,\boldsymbol{S}_\chi^t\right] : \boldsymbol{g}\,\dot{\boldsymbol{F}} - \boldsymbol{\tau}_\chi : \boldsymbol{\epsilon}\cdot\dot{\boldsymbol{\alpha}} \geq 0$$

4. Coleman-Noll procedure

$$\boldsymbol{N}_\chi := \boldsymbol{F}_\chi\,\boldsymbol{S}_\chi^t \qquad \boldsymbol{\tau}_\chi := \boldsymbol{F}\,\boldsymbol{S}_\chi\,\boldsymbol{F}_\chi^t$$

Reorientation equations

1. Orientational non-equilibrium stress equation (solved on element level)

$$\boxed{-\frac{1}{2}\,\boldsymbol{\epsilon} : \boldsymbol{\tau}_\chi = \boldsymbol{\Sigma}_\chi} \qquad \boldsymbol{\Sigma}_\chi = V_\chi\,\dot{\boldsymbol{\alpha}} \qquad \mathcal{D}_\chi^{\mathrm{int}} := 2\,\boldsymbol{\Sigma}_\chi\cdot\dot{\boldsymbol{\alpha}} \geq 0$$

2. Global orientation equation with Dirichlet boundary conditions in general

$$\boxed{\dot{\boldsymbol{\chi}} = -\boldsymbol{\epsilon}\cdot\dot{\boldsymbol{\alpha}}\cdot\boldsymbol{\chi}}$$

Variational-based weak formulation (I)

Principle of virtual power extended to mixed fields

1. Incremental principle of virtual power

$$\int_{t_n}^{t_{n+1}} \delta_* \dot{\mathcal{H}}(\dot{\tilde{\boldsymbol{U}}}_1, \ldots \dot{\tilde{\boldsymbol{U}}}_s, \tilde{\boldsymbol{V}}_1, \ldots \tilde{\boldsymbol{V}}_p)\,\mathrm{d}t = 0$$

2. Virtual power of two global fields: deformation φ and orientation $\boldsymbol{\chi}$

$$\delta_* \dot{\mathcal{H}} := \delta_* \mathcal{P}_\varphi + \delta_* \mathcal{P}_\chi \qquad \mathcal{H} := \mathcal{T} + \Pi^{\mathrm{int}} + \Pi^{\mathrm{ext}}$$

Virtual power associated with the motion (I)

1. Virtual power of motion

$$\delta_* \mathcal{P}_\varphi := \delta_* \dot{\mathcal{T}}_\varphi(\dot{\boldsymbol{\varphi}}, \dot{\boldsymbol{v}}, \dot{\boldsymbol{p}}) + \delta_* \dot{\Pi}_\varphi^{\mathrm{ext}}(\dot{\boldsymbol{\varphi}}, \tilde{\boldsymbol{R}}) + \delta_* \dot{\Pi}_\varphi^{\mathrm{int}}(\dot{\boldsymbol{\varphi}}, \dot{\tilde{\boldsymbol{F}}}, \dot{\tilde{\boldsymbol{C}}}, \tilde{\boldsymbol{P}}, \tilde{\boldsymbol{S}})$$

2. Path-independent virtual kinetic power

$$\delta_* \dot{\mathcal{T}}_\varphi(\dot{\boldsymbol{\varphi}}, \dot{\boldsymbol{v}}, \dot{\boldsymbol{p}}) := \int_{\mathscr{B}_0} \delta_* \dot{\boldsymbol{v}} \cdot [\rho_0\, \boldsymbol{v} - \boldsymbol{p}]\,\mathrm{d}V + \int_{\mathscr{B}_0} \delta_* \dot{\boldsymbol{p}} \cdot [\dot{\boldsymbol{\varphi}} - \boldsymbol{v}]\,\mathrm{d}V + \int_{\mathscr{B}_0} \delta_* \dot{\boldsymbol{\varphi}} \cdot \dot{\boldsymbol{p}}\,\mathrm{d}V$$

3. Path-(in)dependent virtual external power

$$\delta_* \dot{\Pi}_\varphi^{\mathrm{ext}}(\dot{\boldsymbol{\varphi}}, \tilde{\boldsymbol{R}}) := -\int_{\mathscr{B}_0} \delta_* \dot{\boldsymbol{\varphi}} \cdot \boldsymbol{B}\,\mathrm{d}V - \int_{\partial_T \mathscr{B}_0} \delta_* \dot{\boldsymbol{\varphi}} \cdot \bar{\boldsymbol{T}}\,\mathrm{d}A - \int_{\partial_\varphi \mathscr{B}_0} \delta_* \tilde{\boldsymbol{R}} \cdot [\dot{\boldsymbol{\varphi}} - \dot{\bar{\boldsymbol{\varphi}}}]\,\mathrm{d}A - \int_{\partial_\varphi \mathscr{B}_0} \delta_* \dot{\boldsymbol{\varphi}} \cdot \tilde{\boldsymbol{R}}\,\mathrm{d}A$$

Variational-based weak formulation (II)

Introduction
Continuum model
Reorientation
Variational-based weak formulation
Balance laws
Numerical studies
Initial rotation
Boundary load
Volume load
Summary

Virtual power associated with the motion (II)

Path-independent virtual internal power $\delta_* \dot{\Pi}^{\text{int}}_{\varphi}(\dot{\boldsymbol{\varphi}}, \dot{\tilde{\boldsymbol{F}}}, \dot{\tilde{\boldsymbol{C}}}, \tilde{\boldsymbol{P}}, \tilde{\boldsymbol{S}}) := \delta_* \mathcal{P}^{\text{int}}_{\varphi}$

$$\begin{aligned}\delta_* \mathcal{P}^{\text{int}}_{\varphi} := & \int_{\mathscr{B}_0} \delta_* \tilde{\boldsymbol{P}} : \left[\text{Grad}[\dot{\boldsymbol{\varphi}}] - \dot{\tilde{\boldsymbol{F}}}\right] \text{d}V + \frac{1}{2} \int_{\mathscr{B}_0} \delta_* \tilde{\boldsymbol{S}} : \left[\frac{\partial}{\partial t}\left(\tilde{\boldsymbol{F}}^t \tilde{\boldsymbol{F}}\right) - \dot{\tilde{\boldsymbol{C}}}\right] \text{d}V \\ & + \int_{\mathscr{B}_0} \delta_* \dot{\tilde{\boldsymbol{C}}} : \left[\frac{\partial \Psi}{\partial \tilde{\boldsymbol{C}}} - \frac{1}{2}\tilde{\boldsymbol{S}}\right] \text{d}V + \int_{\mathscr{B}_0} \delta_* \dot{\tilde{\boldsymbol{F}}} : \left[\tilde{\boldsymbol{F}}\,\tilde{\boldsymbol{S}} - \tilde{\boldsymbol{P}}\right] \text{d}V + \int_{\mathscr{B}_0} \tilde{\boldsymbol{P}} : \text{Grad}[\delta_* \dot{\boldsymbol{\varphi}}] \, \text{d}V\end{aligned}$$

Virtual power associated with the reorientation (I)

1. Virtual power of orientation

$$\delta_* \mathcal{P}_{\chi} := \delta_* \dot{\mathcal{T}}_{\chi}(\dot{\boldsymbol{\chi}}, \dot{\boldsymbol{v}}_{\chi}, \dot{\boldsymbol{p}}_{\chi}) + \delta_* \mathcal{P}^{\text{ext}}_{\chi} + \delta_* \mathcal{P}^{\text{int}}_{\chi}$$

2. Path-independent virtual kinetic power

$$\begin{aligned}\delta_* \dot{\mathcal{T}}_{\chi}(\dot{\boldsymbol{\chi}}, \dot{\boldsymbol{v}}_{\chi}, \dot{\boldsymbol{p}}_{\chi}) := & \int_{\mathscr{B}_0} \delta_* \dot{\boldsymbol{v}}_{\chi} \cdot \left(\rho_0 \left[(l_{\chi}^2 - l_0^2)\boldsymbol{A}_0 + l_0^2\, \boldsymbol{I}\right] \boldsymbol{v}_{\chi} - \boldsymbol{p}_{\chi}\right) \text{d}V \\ & + \int_{\mathscr{B}_0} \delta_* \dot{\boldsymbol{p}}_{\chi} \cdot [\dot{\boldsymbol{\chi}} - \boldsymbol{v}_{\chi}] \, \text{d}V + \int_{\mathscr{B}_0} \delta_* \dot{\boldsymbol{\chi}} \cdot \dot{\boldsymbol{p}}_{\chi} \, \text{d}V\end{aligned}$$

3. Path-dependent virtual external power $\delta_* \dot{\Pi}^{\text{ext}}_{\chi}(\dot{\boldsymbol{\alpha}}, \dot{\boldsymbol{\chi}}, \tilde{\boldsymbol{Z}}, \tilde{\boldsymbol{\tau}}_n, \tilde{\boldsymbol{\nu}}) =: \delta_* \mathcal{P}^{\text{ext}}_{\chi}$

$$\begin{aligned}\delta_* \mathcal{P}^{\text{ext}}_{\chi} := & -\int_{\mathscr{B}_0} \delta_* \dot{\boldsymbol{\chi}} \cdot \boldsymbol{B}_{\chi} \, \text{d}V - \int_{\partial_W \mathscr{B}_0} \delta_* \dot{\boldsymbol{\chi}} \cdot \bar{\boldsymbol{W}} \, \text{d}A - \int_{\partial_{\chi} \mathscr{B}_0} \delta_* \tilde{\boldsymbol{Z}} \cdot \left[\dot{\boldsymbol{\chi}} - \dot{\bar{\boldsymbol{\chi}}}\right] \text{d}A - \int_{\partial_{\chi} \mathscr{B}_0} \delta_* \dot{\boldsymbol{\chi}} \cdot \tilde{\boldsymbol{Z}} \, \text{d}A \\ & - \int_{\partial_{\chi} \mathscr{B}_0} 2\, \delta_* \tilde{\boldsymbol{\tau}}_n \cdot \tilde{\boldsymbol{\nu}} \, \text{d}A - \int_{\partial_{\chi} \mathscr{B}_0} 2\, \delta_* \tilde{\boldsymbol{\nu}} \cdot \tilde{\boldsymbol{\tau}}_n \, \text{d}A + \int_{\mathscr{B}_0} 2\, \delta_* \dot{\boldsymbol{\alpha}} \cdot \boldsymbol{\Sigma}_{\chi} \, \text{d}V\end{aligned}$$

Introduction
Continuum model
Reorientation
Variational-based weak formulation
Balance laws
Numerical studies
Initial rotation
Boundary load
Volume load
Summary

Variational-based weak formulation (III)

Virtual power associated with the reorientation (II)

Path-independent virtual internal power

$$\delta_* \dot{\varPi}^{\text{int}}_{\chi}(\dot{\boldsymbol{\alpha}}, \dot{\boldsymbol{\chi}}, \dot{\tilde{\boldsymbol{F}}}, \dot{\tilde{\boldsymbol{F}}}_{\chi}, \dot{\tilde{\boldsymbol{G}}}_{\chi}, \dot{\tilde{\boldsymbol{C}}}_{\chi}, \dot{\tilde{\boldsymbol{K}}}_{\chi}, \tilde{\boldsymbol{\tau}}_n, \tilde{\boldsymbol{P}}_{\chi}, \tilde{\boldsymbol{P}}_K, \tilde{\boldsymbol{S}}_{\chi}, \tilde{\boldsymbol{S}}_K) := \delta_* \mathcal{P}^{\text{int}}_{\chi}$$

where

$$\begin{aligned}
\delta_* \mathcal{P}^{\text{int}}_{\chi} := & \int_{\mathscr{B}_0} \delta_* \dot{\tilde{\boldsymbol{F}}} : \left[\tilde{\boldsymbol{F}}_{\chi}\, \tilde{\boldsymbol{S}}^t_{\chi} + \tilde{\boldsymbol{G}}_{\chi}\, \tilde{\boldsymbol{S}}^t_K\right] \mathrm{d}V + \int_{\mathscr{B}_0} 2\, \delta_* \tilde{\boldsymbol{\tau}}_n \cdot [\dot{\boldsymbol{\chi}} + \boldsymbol{\epsilon} \cdot \dot{\boldsymbol{\alpha}} \cdot \boldsymbol{\chi}]\, \mathrm{d}V \\
& + \int_{\mathscr{B}_0} \delta_* \tilde{\boldsymbol{P}}_{\chi} : \left[\dot{\boldsymbol{\chi}} \otimes \boldsymbol{n}_0 - \dot{\tilde{\boldsymbol{F}}}_{\chi}\right] \mathrm{d}V + \int_{\mathscr{B}_0} \delta_* \tilde{\boldsymbol{P}}_K : \left[\mathrm{Grad}[\dot{\boldsymbol{\chi}}] - \dot{\tilde{\boldsymbol{G}}}_{\chi}\right] \mathrm{d}V \\
& + \int_{\mathscr{B}_0} \delta_* \tilde{\boldsymbol{S}}_{\chi} : \left[\frac{\partial}{\partial t}\left(\tilde{\boldsymbol{F}}^t \tilde{\boldsymbol{F}}_{\chi}\right) - \dot{\tilde{\boldsymbol{C}}}_{\chi}\right] \mathrm{d}V + \int_{\mathscr{B}_0} \delta_* \tilde{\boldsymbol{S}}_K : \left[\frac{\partial}{\partial t}\left(\tilde{\boldsymbol{F}}^t \tilde{\boldsymbol{G}}_{\chi}\right) - \dot{\tilde{\boldsymbol{K}}}_{\chi}\right] \mathrm{d}V \\
& + \int_{\mathscr{B}_0} \delta_* \dot{\tilde{\boldsymbol{C}}}_{\chi} : \left[\frac{\partial \Psi}{\partial \tilde{\boldsymbol{C}}_{\chi}} - \tilde{\boldsymbol{S}}_{\chi}\right] \mathrm{d}V + \int_{\mathrm{B}_0} \delta_* \dot{\tilde{\boldsymbol{K}}}_{\chi} : \left[\frac{\partial \Psi}{\partial \tilde{\boldsymbol{K}}_{\chi}} - \tilde{\boldsymbol{S}}_K\right] \mathrm{d}V \\
& + \int_{\mathscr{B}_0} \delta_* \dot{\tilde{\boldsymbol{F}}}_{\chi} : [\tilde{\boldsymbol{F}}\, \tilde{\boldsymbol{S}}_{\chi} - \tilde{\boldsymbol{P}}_{\chi}]\, \mathrm{d}V + \int_{\mathscr{B}_0} \delta_* \dot{\tilde{\boldsymbol{G}}}_{\chi} : [\tilde{\boldsymbol{F}}\, \tilde{\boldsymbol{S}}_K - \tilde{\boldsymbol{P}}_K]\, \mathrm{d}V \\
& + \int_{\mathscr{B}_0} \tilde{\boldsymbol{P}}_{\chi} : [\delta_* \dot{\boldsymbol{\chi}} \otimes \boldsymbol{n}_0]\, \mathrm{d}V + \int_{\mathrm{B}_0} \tilde{\boldsymbol{P}}_K : \mathrm{Grad}[\delta_* \dot{\boldsymbol{\chi}}]\, \mathrm{d}V + \int_{\mathscr{B}_0} \delta_* \tilde{\boldsymbol{S}}_{\chi} : \tilde{\boldsymbol{F}}^t (\boldsymbol{\epsilon} \cdot \boldsymbol{\alpha})\, \tilde{\boldsymbol{F}}_{\chi}\, \mathrm{d}V \\
& + \int_{\mathscr{B}_0} \left[\frac{1}{2} \boldsymbol{\epsilon} : \boldsymbol{\tau}_{\chi} - \tilde{\boldsymbol{\tau}}_n \cdot \boldsymbol{\epsilon} \cdot \boldsymbol{\chi}\right] \cdot 2\, \delta_* \dot{\boldsymbol{\alpha}}\, \mathrm{d}V + \int_{\mathscr{B}_0} 2\, \tilde{\boldsymbol{\tau}}_n \cdot \delta_* \dot{\boldsymbol{\chi}}\, \mathrm{d}V
\end{aligned}$$

Total virtual power in the incremental principle

$$\delta_* \dot{\mathcal{H}} := \delta_* \mathcal{P}_{\varphi} + \delta_* \dot{\mathcal{T}}_{\chi}(\dot{\boldsymbol{\chi}}, \dot{\boldsymbol{v}}_{\chi}, \dot{\boldsymbol{p}}_{\chi}) + \delta_* \mathcal{P}^{\text{ext}}_{\chi} + \delta_* \mathcal{P}^{\text{int}}_{\chi}$$

Introduction
Continuum model
Reorientation
Variational-based weak formulation
Balance laws
Numerical studies
Initial rotation
Boundary load
Volume load
Summary

Main weak forms of motion with reorientation

Weak balance of linear momentum

$$\int_{\mathcal{T}_n}\int_{\mathcal{B}_0} \delta_*\dot{\boldsymbol{\varphi}}\cdot[\dot{\boldsymbol{p}}-\boldsymbol{B}]\,\mathrm{d}V\,\mathrm{d}t - \int_{\mathcal{T}_n}\int_{\partial_T\mathcal{B}_0} \bar{\boldsymbol{T}}\cdot\delta_*\dot{\boldsymbol{\varphi}}\,\mathrm{d}A\,\mathrm{d}t + \int_{\mathcal{T}_n}\int_{\mathcal{B}_0} \tilde{\boldsymbol{P}}:\mathrm{Grad}[\delta_*\dot{\boldsymbol{\varphi}}]\,\mathrm{d}V\,\mathrm{d}t = \int_{\mathcal{T}_n}\int_{\partial_\varphi\mathcal{B}_0} \tilde{\boldsymbol{R}}\cdot\delta_*\dot{\boldsymbol{\varphi}}\,\mathrm{d}A\,\mathrm{d}t$$

Weak balance of orientational momentum

$$\int_{\mathcal{T}_n}\int_{\mathcal{B}_0} \delta_*\dot{\boldsymbol{\chi}}\cdot\left[\dot{\boldsymbol{p}}_\chi + 2\,\tilde{\boldsymbol{\tau}}_n - \boldsymbol{B}_\chi\right]\mathrm{d}V\,\mathrm{d}t - \int_{\mathcal{T}_n}\int_{\partial_W\mathcal{B}_0} \bar{\boldsymbol{W}}\cdot\delta_*\dot{\boldsymbol{\chi}}\,\mathrm{d}A\,\mathrm{d}t + \int_{\mathcal{T}_n}\int_{\mathcal{B}_0} \tilde{\boldsymbol{P}}_K:\mathrm{Grad}[\delta_*\dot{\boldsymbol{\chi}}]\,\mathrm{d}V\,\mathrm{d}t + \int_{\mathcal{T}_n}\int_{\mathcal{B}_0} \tilde{\boldsymbol{P}}_\chi:[\delta_*\dot{\boldsymbol{\chi}}\otimes\boldsymbol{n}_0]\,\mathrm{d}V\,\mathrm{d}t = \int_{\mathcal{T}_n}\int_{\partial_\chi\mathcal{B}_0} \tilde{\boldsymbol{Z}}\cdot\delta_*\dot{\boldsymbol{\chi}}\,\mathrm{d}A\,\mathrm{d}t$$

Weak balance of orientation rate

$$\int_{\mathcal{T}_n}\int_{\mathcal{B}_0} 2\,\delta_*\tilde{\boldsymbol{\tau}}_n\cdot[\dot{\boldsymbol{\chi}}+\boldsymbol{\epsilon}\cdot\dot{\boldsymbol{\alpha}}\cdot\boldsymbol{\chi}]\,\mathrm{d}V\,\mathrm{d}t = \int_{\mathcal{T}_n}\int_{\partial_\chi\mathcal{B}_0} 2\,\delta_*\tilde{\boldsymbol{\tau}}_n\cdot\tilde{\boldsymbol{\nu}}\,\mathrm{d}A\,\mathrm{d}t$$

Weak balance of reorientation stress (locally/element-wise solved)

$$\int_{\mathcal{T}_n}\int_{\mathcal{B}_\square} 2\,\delta_*\dot{\boldsymbol{\alpha}}\cdot\left[\tilde{\boldsymbol{\tau}}_n\times\boldsymbol{\chi} + \frac{1}{2}\,\boldsymbol{\epsilon}:\boldsymbol{\tau}_\chi + \boldsymbol{\Sigma}_\chi\right]\mathrm{d}\square\,\mathrm{d}t = 0$$

Introduction

Continuum model

Reorientation

Variational-based weak formulation

Balance laws

Numerical studies

Initial rotation

Boundary load

Volume load

Summary

Balance laws of the weak formulation (I)

Energy and momentum functions of the LCE extended continuum

Kinetic energy $\mathcal{T}(t) := \int_{\mathscr{B}_0} \frac{1}{2}\boldsymbol{v}\cdot\boldsymbol{p}\,\mathrm{d}V$	Kinetic energy of orientation $\mathcal{T}_\chi(t) := \int_{\mathscr{B}_0} \frac{1}{2}\boldsymbol{v}_\chi\cdot\boldsymbol{p}_\chi\,\mathrm{d}V$	Potential energy $\Pi^{\mathrm{int}}(t) := \int_{\mathscr{B}_0} \Psi\,\mathrm{d}V$
Linear momentum $\boldsymbol{L}(t) := \int_{\mathscr{B}_0} \boldsymbol{p}\,\mathrm{d}V$	Angular momentum $\boldsymbol{J}(t) := \int_{\mathscr{B}_0} \boldsymbol{\varphi}\times\boldsymbol{p}\,\mathrm{d}V$	Momentum of orientation $\boldsymbol{L}_\chi(t) := \int_{\mathscr{B}_0} \boldsymbol{p}_\chi\,\mathrm{d}V$
Moment of momentum $\boldsymbol{J}_\chi(t) := \int_{\mathscr{B}_0} \boldsymbol{\chi}\times\boldsymbol{p}_\chi\,\mathrm{d}V$	Reorientation function $\mathcal{C}^{\mathrm{ori}}(t) := \int_{\mathscr{B}_0} \left[\|\boldsymbol{\chi}\|^2 - 1\right]\mathrm{d}V$	Total energy $\mathcal{H} := \mathcal{T} + \mathcal{T}_\chi + \Pi^{\mathrm{int}} + \Pi^{\mathrm{ext}}$

Linear momentum

(symmetry of virtual translations)

$$\boldsymbol{L}(t_{n+1}) - \boldsymbol{L}(t_n) = \int_{\mathscr{T}_n}\int_{\mathscr{B}_0} \boldsymbol{B}\,\mathrm{d}V\,\mathrm{d}t + \int_{\mathscr{T}_n}\int_{\partial_T\mathscr{B}_0} \bar{\boldsymbol{T}}\,\mathrm{d}A\,\mathrm{d}t + \int_{\mathscr{T}_n}\int_{\partial_\varphi\mathscr{B}_0} \tilde{\boldsymbol{R}}\,\mathrm{d}A\,\mathrm{d}t$$

Orientational momentum

(symmetry of virtual orientations)

$$\boldsymbol{L}_\chi(t_{n+1}) - \boldsymbol{L}_\chi(t_n) = \int_{\mathscr{T}_n}\int_{\mathscr{B}_0} [\boldsymbol{B}_\chi - 2\,\tilde{\boldsymbol{\tau}}_n - \tilde{\boldsymbol{P}}_\chi\,\boldsymbol{n}_0]\,\mathrm{d}V\,\mathrm{d}t + \int_{\mathscr{T}_n}\int_{\partial_W\mathscr{B}_0} \bar{\boldsymbol{W}}\,\mathrm{d}A\,\mathrm{d}t + \int_{\mathscr{T}_n}\int_{\partial_\chi\mathscr{B}_0} \tilde{\boldsymbol{Z}}\,\mathrm{d}A\,\mathrm{d}t$$

Introduction

Continuum model

Reorientation

Variational-based weak formulation

Balance laws

Numerical studies

Initial rotation

Boundary load

Volume load

Summary

Balance laws of the weak formulation (II)

Angular momentum (symmetry of virtual rotations)

$$\boldsymbol{J}(t_{n+1}) - \boldsymbol{J}(t_n) = \int_{\mathcal{T}_n}\int_{\mathcal{B}_0} \boldsymbol{\varphi} \times \boldsymbol{B}\,\mathrm{d}V\,\mathrm{d}t + \int_{\mathcal{T}_n}\int_{\partial_T\mathcal{B}_0} \boldsymbol{\varphi} \times \bar{\boldsymbol{T}}\,\mathrm{d}A\,\mathrm{d}t + \int_{\mathcal{T}_n}\int_{\partial_\varphi\mathcal{B}_0} \boldsymbol{\varphi} \times \tilde{\boldsymbol{R}}\,\mathrm{d}A\,\mathrm{d}t + \int_{\mathcal{T}_n}\int_{\mathcal{B}_0} [\tilde{\boldsymbol{F}}_\chi \tilde{\boldsymbol{S}}_\chi^t + \tilde{\boldsymbol{G}}_\chi \tilde{\boldsymbol{S}}_K^t] \times \tilde{\boldsymbol{F}}\,\mathrm{d}V\,\mathrm{d}t$$

Moment of orientational momentum (symmetry of virtual reorientations)

$$\boldsymbol{J}_\chi(t_{n+1}) - \boldsymbol{J}_\chi(t_n) = \int_{\mathcal{T}_n}\int_{\mathcal{B}_0} \boldsymbol{\chi} \times \boldsymbol{B}_\chi\,\mathrm{d}V\,\mathrm{d}t + \int_{\mathcal{T}_n}\int_{\partial_W\mathcal{B}_0} \boldsymbol{\chi} \times \bar{\boldsymbol{W}}\,\mathrm{d}A\,\mathrm{d}t + \int_{\mathcal{T}_n}\int_{\partial_\chi\mathcal{B}_0} \boldsymbol{\chi} \times \tilde{\boldsymbol{Z}}\,\mathrm{d}A\,\mathrm{d}t - \int_{\mathcal{T}_n}\int_{\mathcal{B}_0} [\tilde{\boldsymbol{F}}_\chi \tilde{\boldsymbol{S}}_\chi^t + \tilde{\boldsymbol{G}}_\chi \tilde{\boldsymbol{S}}_K^t] \times \tilde{\boldsymbol{F}}\,\mathrm{d}V\,\mathrm{d}t - \int_{\mathcal{T}_n}\int_{\mathcal{B}_0} \boldsymbol{\chi} \times 2\,\tilde{\boldsymbol{\tau}}_n\,\mathrm{d}V\,\mathrm{d}t$$

Kinetic energy of motion (symmetry of virtual time shifts)

$$\mathcal{T}(t_{n+1}) - \mathcal{T}(t_n) = \int_{\mathcal{T}_n}\int_{\mathcal{B}_0} \boldsymbol{B} \cdot \dot{\boldsymbol{\varphi}}\,\mathrm{d}V\,\mathrm{d}t + \int_{\mathcal{T}_n}\int_{\partial_T\mathcal{B}_0} \bar{\boldsymbol{T}} \cdot \dot{\boldsymbol{\varphi}}\,\mathrm{d}A\,\mathrm{d}t + \int_{\mathcal{T}_n}\int_{\partial_\varphi\mathcal{B}_0} \tilde{\boldsymbol{R}} \cdot \dot{\boldsymbol{\varphi}}\,\mathrm{d}A\,\mathrm{d}t - \int_{\mathcal{T}_n}\int_{\mathcal{B}_0} [\tilde{\boldsymbol{S}} : \dot{\boldsymbol{F}}^t \tilde{\boldsymbol{F}} + \tilde{\boldsymbol{S}}_\chi : \dot{\boldsymbol{F}}^t \tilde{\boldsymbol{F}}_\chi + \tilde{\boldsymbol{S}}_K : \dot{\boldsymbol{F}}^t \tilde{\boldsymbol{G}}_\chi]\,\mathrm{d}V\,\mathrm{d}t$$

Kinetic energy of orientation (symmetry of virtual time shifts)

$$\mathcal{T}_\chi(t_{n+1}) - \mathcal{T}_\chi(t_n) = \int_{\mathcal{T}_n}\int_{\mathcal{B}_0} \boldsymbol{B}_\chi \cdot \dot{\boldsymbol{\chi}}\,\mathrm{d}V\,\mathrm{d}t + \int_{\mathcal{T}_n}\int_{\partial_\varphi\mathcal{B}_0} \bar{\boldsymbol{W}} \cdot \dot{\boldsymbol{\chi}}\,\mathrm{d}A\,\mathrm{d}t + \int_{\mathcal{T}_n}\int_{\partial_\varphi\mathcal{B}_0} \tilde{\boldsymbol{Z}} \cdot \dot{\boldsymbol{\chi}}\,\mathrm{d}A\,\mathrm{d}t - \int_{\mathcal{T}_n}\int_{\mathcal{B}_0} [\tilde{\boldsymbol{S}}_\chi : \tilde{\boldsymbol{F}}^t \left(\dot{\boldsymbol{F}}_\chi + \boldsymbol{\epsilon} \cdot \dot{\boldsymbol{\alpha}} \cdot \tilde{\boldsymbol{F}}_\chi\right) + \tilde{\boldsymbol{S}}_K : \tilde{\boldsymbol{F}}^t \dot{\boldsymbol{G}}_\chi + D_\chi^{\mathrm{int}}]\,\mathrm{d}V\,\mathrm{d}t$$

Introduction

Continuum model

Reorientation

Variational-based weak formulation

Balance laws

Numerical studies

Initial rotation

Boundary load

Volume load

Summary

Balance laws of the weak formulation (III)

Path-independent volume dead loads

$$\Pi^{\text{ext}}(t) := -\int_{\mathscr{B}_0} \boldsymbol{B}\cdot\boldsymbol{\varphi}\,\mathrm{d}V\,\mathrm{d}t - \int_{\mathscr{B}_0} \boldsymbol{B}_\chi\cdot\boldsymbol{\chi}\,\mathrm{d}V$$

Potential energy

(symmetry of virtual time shifts)

$$\Pi(t_{n+1}) - \Pi(t_n) = \int_{\mathscr{T}_n}\int_{\mathscr{B}_0}[\tilde{\boldsymbol{S}}_\chi : \frac{\partial}{\partial t}\Big(\tilde{\boldsymbol{F}}^t\tilde{\boldsymbol{F}}_\chi\Big) + \tilde{\boldsymbol{S}}_K : \frac{\partial}{\partial t}\Big(\tilde{\boldsymbol{F}}^t\tilde{\boldsymbol{G}}_\chi\Big) + \tilde{\boldsymbol{S}}_\chi : \tilde{\boldsymbol{F}}^t(\boldsymbol{\epsilon}\cdot\dot{\boldsymbol{\alpha}})\tilde{\boldsymbol{F}}_\chi]\,\mathrm{d}V\mathrm{d}t$$
$$+ \int_{\mathscr{T}_n}\int_{\mathscr{B}_0}\Big[\tilde{\boldsymbol{S}} : \dot{\tilde{\boldsymbol{F}}}^t\tilde{\boldsymbol{F}} - \boldsymbol{B}\cdot\dot{\boldsymbol{\varphi}} - \boldsymbol{B}_\chi\cdot\dot{\boldsymbol{\chi}}\Big]\,\mathrm{d}V\mathrm{d}t$$

Total energy

(symmetry of virtual time shifts)

$$\mathcal{H}(t_{n+1}) - \mathcal{H}(t_n) = \int_{\mathscr{T}_n}\int_{\partial_\varphi\mathscr{B}_0}\tilde{\boldsymbol{R}}\cdot\dot{\boldsymbol{\varphi}}\,\mathrm{d}A\,\mathrm{d}t + \int_{\mathscr{T}_n}\int_{\partial_\varphi\mathscr{B}_0}\tilde{\boldsymbol{Z}}\cdot\dot{\boldsymbol{\chi}}\,\mathrm{d}A\,\mathrm{d}t$$
$$- \int_{\mathscr{T}_n}\int_{\partial_T\mathscr{B}_0}\bar{\boldsymbol{T}}\cdot\dot{\boldsymbol{\varphi}}\,\mathrm{d}A\,\mathrm{d}t + \int_{\mathscr{T}_n}\int_{\partial_\varphi\mathscr{B}_0}\bar{\boldsymbol{W}}\cdot\dot{\boldsymbol{\chi}}\,\mathrm{d}A\,\mathrm{d}t - \int_{\mathscr{T}_n}\int_{\partial_\varphi\mathscr{B}_0} D_\chi^{\text{int}}\,\mathrm{d}A\,\mathrm{d}t$$

Reorientation function

$$\mathcal{C}^{\text{ori}}(t_{n+1}) - \mathcal{C}^{\text{ori}}(t_n) \equiv \int_{\mathscr{T}_n}\int_{\mathscr{B}_0} 2\,\boldsymbol{\chi}\cdot\dot{\boldsymbol{\chi}}\,\mathrm{d}V\,\mathrm{d}t = \int_{\mathscr{T}_n}\int_{\partial_\chi\mathscr{B}_0} 2\,\boldsymbol{\chi}\cdot\tilde{\boldsymbol{\nu}}\,\mathrm{d}A\,\mathrm{d}t$$

Introduction
Continuum model
Reorientation
Variational-based weak formulation
Balance laws
Numerical studies
Initial rotation
Boundary load
Volume load
Summary

Thin LCE strip subject to initial rotation

Boundary and initial conditions

121-em with H20-mixed-Bbar

Mesh and boundary conditions

$\boldsymbol{n}_0^A = \boldsymbol{e}_y,\ \boldsymbol{\omega}_0^A = 32\,\boldsymbol{e}_z[1/\mathrm{s}]$

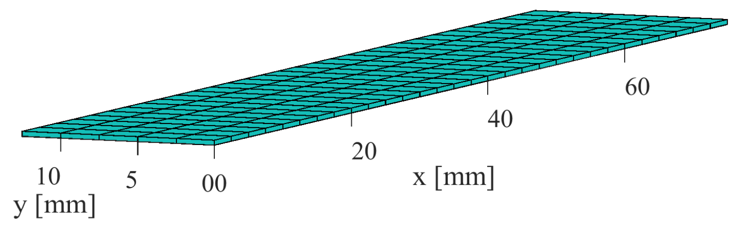

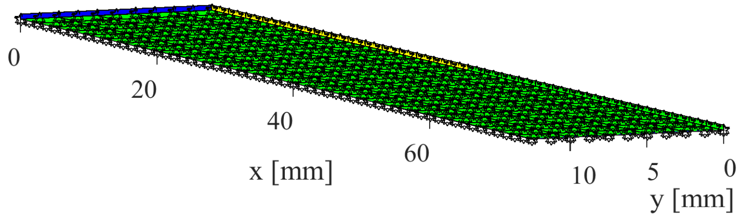

Activated Dirichlet and Neumann boundaries

Green bottom patches as boundary $\partial_\chi \mathcal{B}_0$: Fixed orientation $n_z^A = 0$

Thin LCE strip subject to initial rotation

Dynamic effects of the reorientation

Balance laws with/without reorientation $(\mathrm{E} \approx 0.914\,[\mathrm{MPa}],\ \nu \approx 0.493)$

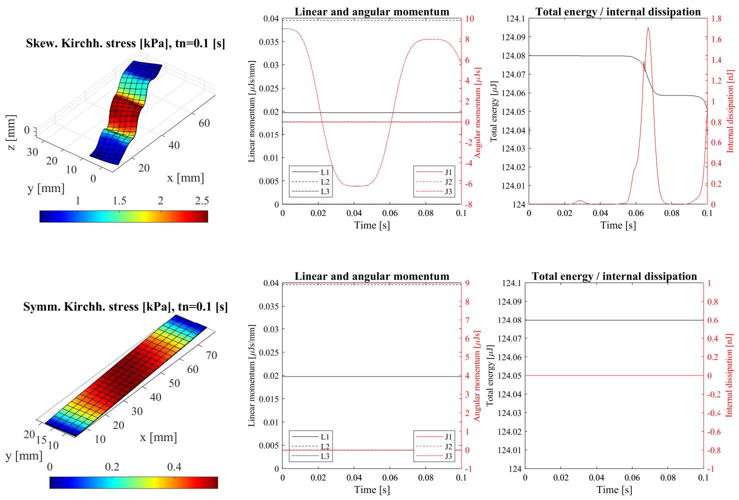

Introduction
Continuum model
Reorientation
Variational-based weak formulation
Balance laws
Numerical studies
Initial rotation
Boundary load
Volume load
Summary

Thin LCE strip subject to initial rotation

Unsteady right-left-rotation due to reorientation

Movie of the soft strip ($E \approx 0.914\,[\mathrm{MPa}]$, $\nu \approx 0.493$)

Thin LCE strip subject to initial rotation

Unsteady right-left-rotation due to reorientation

Balance laws versus time $(E \approx 0.914\,[\mathrm{MPa}],\ \nu \approx 0.493)$

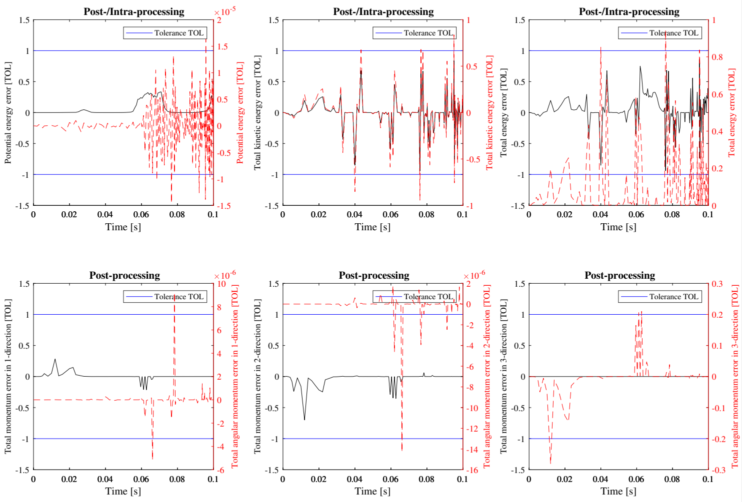

Thin LCE strip subject to boundary load

Boundary and initial conditions

121-em with H20-mixed-Bbar

Boundary conditions and loads

$\boldsymbol{n}_0 = (\boldsymbol{e}_x + \boldsymbol{e}_y)/\sqrt{2}$

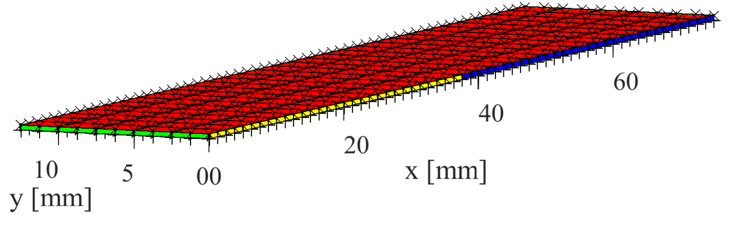

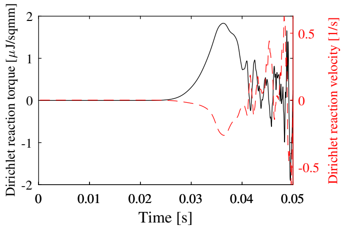

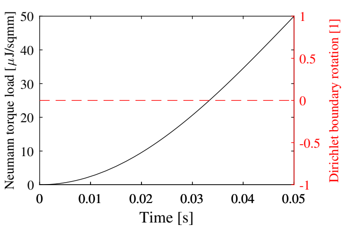

Activated Dirichlet and Neumann boundaries

Red top as $\partial_W \mathcal{B}_0$: $W_y^A = -\hat{W}^A(t)$ Green bottom as $\partial_\chi \mathcal{B}_0$: Fixed orientation $n_z^A = 0$

Thin LCE strip subject to boundary load

Contraction with folding motion

Movie of the stiffer strip $(\mathrm{E} \approx 9.140\,[\mathrm{MPa}],\ \nu \approx 0.493)$

Introduction
Continuum model
Reorientation
Variational-based weak formulation
Balance laws
Numerical studies
Initial rotation
Boundary load
Volume load
Summary

Introduction
Continuum model
Reorientation
Variational-based weak formulation
Balance laws
Numerical studies
Initial rotation
Boundary load
Volume load
Summary

Thin LCE strip subject to volume load

Boundary and initial conditions

121-em with H20-mixed-Bbar

Boundary conditions and loads

$\boldsymbol{n}_0 = \boldsymbol{e}_x$

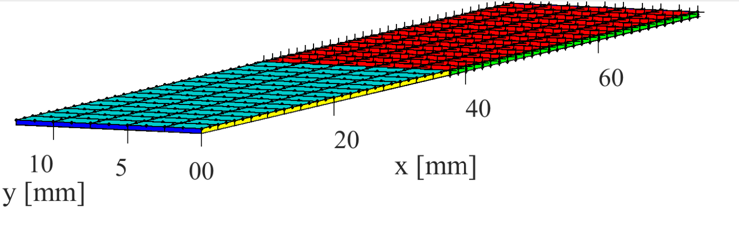

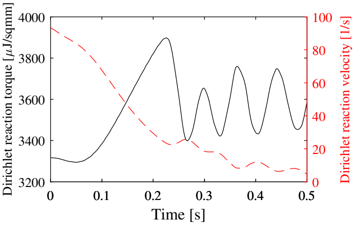

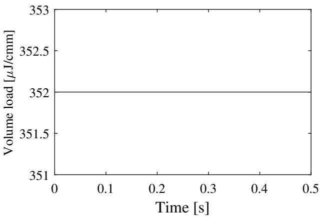

Activated Dirichlet and Neumann boundaries

Red top as $\partial_\chi \mathcal{B}_0$: Fixed orientation $\boldsymbol{n}^A = \boldsymbol{n}_0^A$ $\quad \boldsymbol{n}_0^A = \boldsymbol{e}_x$ $\quad \boldsymbol{B}_\chi = \rho_0 \, B \, (-\boldsymbol{e}_z)$

Thin LCE strip subject to volume load

Steady clockwise rotation due to reorientation

Movie of the stiffer strip ($\mathrm{E} \approx 9.140\,[\mathrm{MPa}]$, $\nu \approx 0.493$)

A VARIATIONAL-BASED MIXED FINITE ELEMENT FORMULATION FOR LIQUID CRYSTAL ELASTOMERS

Groß M., Dietzsch J. and Concas F.

Introduction

Continuum model

Reorientation

Variational-based weak formulation

Balance laws

Numerical studies

Initial rotation

Boundary load

Volume load

Summary

Thin LCE strip subject to volume load

Steady clockwise rotation due to reorientation

Nodal time evolutions and balance laws $(E \approx 9.140\,[\mathrm{MPa}],\ \nu \approx 0.493)$

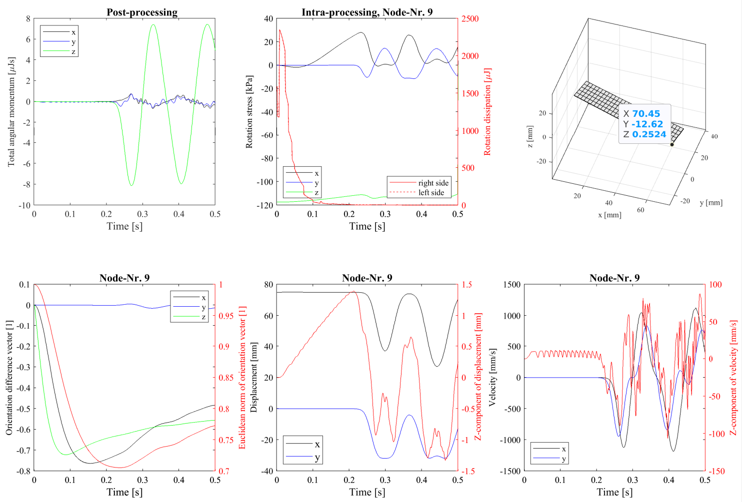

Introduction
Continuum model
Reorientation
Variational-based weak formulation
Balance laws
Numerical studies
Initial rotation
Boundary load
Volume load
Summary

Summary

1. Motivation: Simulations of motion actuations
   - with liquid crystal elastomer materials as actuators by using of
   - boundary and volume loads (thermal and photochemical fields).
2. Goals: Dynamic FE simulations
   - with the approach of a mixed finite element method and
   - reorientations by using of drilling degrees of freedom.
3. Strategy:
   - Introduction of an independent global orientation field,
   - Formulation of local rotation by drilling degrees of freedom,
   - Using of local evolution equations for stress-induced motions.
4. Results: Motion actuation
   - with Neumann boundary loads and volume-specific loads,
   - which activates deformation modes and rigid-body modes.
5. Next step:
   - Thermo-mechanical coupling for simulating thermal actuations